Hemostatic Gelatin-Alginate Hydrogels Modified with Humic Acids and Impregnated with Aminocaproic Acid

Vladimir Lebedev[1,*], Katerina Lebedeva[1], Anna Cherkashina[1], Sergey Petrushenko[2,3], Sergiy Bogatyrenko[2], Anzhela Olkhovska[4], Ihor Hrubnyk[5], Liudmyla Maloshtan[5], Volodymyr Kopach[6] and Natalja Klochko[6]

[1]*The Department of Plastics and Biologically Active Polymers Technology, National Technical University «Kharkiv Polytechnic Institute», 2, Kyrpychova str., 61002 Kharkiv, Ukraine*

[2]*Faculty of Physics, V.N. Karazin Kharkiv National University, 4, Svobody Square, 61022, Kharkiv, Ukraine*

[3]*Technical University of Liberec, 2, Studentska str., 46117, Liberec, Czech Republic Technical University of Liberec, 46117 Liberec, Czech Republic*

[4]*The Department of Organizations and Management Healthcare and Social Medicine, National Technical University «Kharkiv Polytechnic Institute», 2, Kyrpychova str., 61002 Kharkiv, Ukraine*

[5]*The Common Pharmacy Department, National Technical University «Kharkiv Polytechnic Institute», 2, Kyrpychova str., 61002 Kharkiv, Ukraine*

[6]*Department of Micro- and Nanoelectronics, National Technical University «Kharkiv Polytechnic Institute», 2, Kyrpychova str., 61002 Kharkiv, Ukraine*

Abstract: The work is devoted to the development of safe and biocompatible multicomponent gelatin-alginate hydrogels modified with humic acids (HA) and impregnated with the antifibrinolytic agent aminocaproic acid (AA).These hydrogels are designed to be effective hemostatic materials with anti-inflammatory properties and the ability to deliver in less than 30 seconds to deep and hidden areas of hemorrhages. Studies of the crystal structure by X-ray diffraction analysis and non-covalent interactions of molecules by Fourier transform infrared spectroscopy of the developed hemostatic gelatin-alginate hydrogels modified with bactericidal and anti-inflammatory humic acids made it possible to identify the optimal concentrations of HA from 2.5 wt.%. up to 5 wt.%. At such concentrations of HA, gelatin-alginate hydrogels have a semicrystalline structure. Due to non-covalent bonds between polymer chains, they are thermo-responsive with a gel-sol transition temperature of about 37 °C. Impregnation of these hydrogels with aminocaproic acid led to an almost threefold increase in their swelling, which facilitated the dissolution of AA in the hydrogels and its subsequent delivery to the wound. Experiments simulating the transmembrane transport of aminocaproic acid from the developed gelatin-alginate hydrogels confirmed their ability to rapidly deliver up to 494± 3 mg of AA from 5 ml of hydrogel to the wound.

Keywords: Hemostasis, biopolymer hydrogel, swelling, thermo-responsivity, drug delivery, X-ray diffractometry, Fourier transform infrared spectroscopy, transmembrane transport.

1. INTRODUCTION

Trauma, both on the battlefield and in civilian settings, is a leading cause of death worldwide, as uncontrolled bleeding from traumatic injury causes many complications, including hypothermia, coagulopathy, wound infection, acidosis, and multiple organ failure [1-6]. The loss of more than one-third of the body's blood causes a number of systemic reactions, such as deep coma and shock [5]. According to Jiao *et al.* (2023), with severe post-traumatic bleeding, the mortality rate is 30–40%, with about half of such patients dying before hospitalization. Hemorrhage is one of the most serious threats to life on the battlefield, accounting for 50% of the total lethal outcomes, and almost 86% of combat casualties occur within the first 30 minutes after wounding [6]. Fortunately, death caused by severe bleeding can be prevented by achieving prompt and efficient hemostasis. Studies have shown [5] that if bleeding can be stopped within 60 minutes, the victim's survival rate increases by 20–30%.

Hemostasis is a complex process that includes two stages: primary hemostasis and secondary hemostasis (coagulation cascade) [3, 6, 7]. During primary hemostasis, vasoconstriction is caused by contraction of vascular smooth muscle to reduce blood loss from the wound. At the same time, secreted procoagulant proteins and platelet factors are activated, adhere and aggregate at the site of injury, forming soft platelet plugs. At this stage, the rapid and abundant absorption of water from the blood by hemostatic agents such as powders or hydrogels promotes the aggregation of

*Address correspondence to this author at the National Technical University «Kharkiv Polytechnic Institute», 2, Kyrpychova str., 61002 Kharkiv, Ukraine; Tel: +380669213261; E-mail: vladimirlebedev1980@ukr.net

E-ISSN: 1929-5995/24

blood cells and platelets to enhance hemostasis as they exert a tamponade effect to stop bleeding [8]. The above primary hemostasis provides a short-term effect. The secondary hemostasis stage is the process of forming fibrin clotting via multiple intermediate steps and employing a precursor called fibrinogen at the site of initial hemostatic plug. The fibrin is used to bolster the platelet plug that is formed in the primary hemostasis stage. According to Yu and Zhong (2021), there are two ways of functioning of hemostatic materials: namely the active path and the passive path. The active pathway triggers the primary and secondary hemostasis described above with a specific effect of initiation of the blood coagulation cascade, whereas the passive pathway provides hemostasis due to hemocompatibility and anti-inflammatory properties of hemostatic agents.

Currently, commercially available hemostatic materials include inorganic substances such as zeolite, silica, montmorillonite and kaolin powders, as well as polymer-based hemostatic materials, including oxidized cellulose, collagen, gelatin (GN), chitosan, silk fibroin, alginate (ALG), fibrin, keratin, thrombin, fibrinogen, starch, polyethylene glycol, cyanoacrylate, etc. [1,6,7,9,10,11]. However, some of them have disadvantages such as high cost, limited hemostatic or antibacterial effect, poor biodegradability and susceptibility to immune reactions [3, 6, 7, 9, 10, 11]. For example, according to Xie *et al*. (2022), the low active pH of oxidized cellulose, around 3.1, makes it cytotoxic and inactivates many biologically active ingredients, which limits its use on sensitive tissues. Fibrin, thrombin and fibrinogen have a short shelf life and a risk of disease transmission [9]. Zeolites release a large amount of heat when they absorb water from blood, causing thermal damage and necrosis of surrounding tissues [9]. Moreover, individual immune systems may reject some hemostatic materials or lead to thrombosis due to excessive blood clotting, which can be fatal [6].According to Chen*et al*. (2023), Li *et al*. (2020), Zhong *et al*. (2021), Jiao *et al*. (2023), Yang *et al*. (2024), Ghimire *et al*. (2021), current hemostatic materials or methods cannot provide safe and effective hemostasis, since, for example, their ability to access the source of bleeding in the amount necessary for blood clotting is limited or hemostatic materials have poor biocompatibility. This is especially important for bleeding wounds of irregular external and internal shape, located deep in complex and hidden areas of hemorrhage, when simply using a tourniquet or gauze cannot work [1, 2, 5, 6].

Therefore, the development of new hemostatic materials is of great interest, and significant interdisciplinary research efforts are required to conduct robust studies aimed at creating ideal hemostatic agents. In accordance with Zhong *et al*. (2021), Ghimire *et al*. (2021), Yu and Zhong (2021), an ideal hemostatic material has the following properties: the ability to deliver a hemostatic agent in less than 30 seconds and stop bleeding within 2 minutes; sufficient biodegradability, non-cytotoxicity and bioabsorbability; clinical safety; ease of use and low cost. Due to the limited hemostatic properties of single-component hemostatic materials, it is necessary to develop composite hemostatic materials containing multiple active hemostatic agents to improve their hemostatic properties. Therefore, the current trend is to combine different materials to obtain an ideal hemostatic product [3, 7, 12, 14].

In recent years, biopolymers have been increasingly used in hemostatic agents such as medical dressings, adhesive hemostatic microneedles, injection hydrogels and hemostatic powders [8-15]. Among them, gelatin due to its excellent characteristics, such a slow antigenicity, availability, biocompatibility, and biodegradability yields hemostasis not only by activating and aggregating blood platelets but also by blocking the gash, as dry gelatin powder has the capacity of swelling up to 200%invivoupon contact with blood, forming a structural hydrogel matrix for blood clotting [3,6]. To improve the thermal and mechanical stability of gelatin, it is advisable [3, 6, 15] to use chemical cross-linking agents to react with the amino groups in gelatin, for example, combining GN with another suitable hemostatic material. Alginate is one such hemostatic biopolymer, and there has been continuous progress in the preparation and research of alginate stimulus-responsive hydrogels [9, 13] as well as thermo-responsive gelatin-alginate hydrogels [12, 14]. According to Zhong *et al*. (2021), Xie *et al*. (2022), the excellent biocompatibility of alginate, its biodegradability, non-toxicity, non-immunogenicity, availability, high water absorption and rapid gelation make ALG dressings particularly suitable for healing of exuding wounds.

In this work, in order to develop an effective hemostatic material, we study thermo-responsive gelatin-alginate hydrogels having temperature of gel-sol transitionnear to physiological temperature 37^{o}C. This allows hydrogels to soften and melt when applied to the surface of the human body and penetrate deep into bleeding wounds of irregular external and internal

shape, absorbing large amounts of water from the blood due to the rapid swelling of hydrogels, as well as triggering coagulation cascade due to the active hemostatic properties of gelatin and alginate. These GN-ALG hydrogels were modified with humic acids (HA) as antioxidant, antibacterial, fungicidal and anti-inflammatory agents for passive hemostasis, which, according to Venezia *et al*. (2022), can also regulate the gelation of gelatin hydrogels.

In addition, since the rapid formation of fibrin at the site of bleeding can be promoted by antifibrinolysis, which enhances the hemostatic effect [5], aminocaproic acid (AA) was added to these hydrogels. Aminocaproic acid (ε-aminocaproic acid,6-aminohexanoic acid, $C_6H_{13}NO_2$) is a synthetic antifibrinolytic drug that inhibits the activation of plasminogen, thereby delaying the degradation of blood clots and subsequently reducing blood loss [1], which has long been used in clinical practice as a broad-spectrum hemostatic agent [16-18]. Recently, the authors Chen*et al*. (2023) developed a biocompatible and biodegradable biopolymer derivative of chitosan grafted with aminocaproic acid, which has antibacterial and hemostatic properties that prevent secondary bleeding, since dissociated AA exhibits antiplasmin activity, slowing down the destruction of blood clots and reducing secondary wound bleeding.

Considering the outstanding hemostatic properties of gelatin, alginate and humic acids noted above, this work studied the crystal structure, intermolecular bonds and swelling properties of hemostatic gelatin-alginate hydrogels modified with humic acids in order to determine the range of optimal HA concentrations. The equilibrium degree of swelling within 30 seconds of these aminocaproic acid-impregnated hydrogels was then studied and the delivery of AA from them to the wound site at physiological temperature was experimentally simulated to confirm their suitability for rapid and efficient hemostasis.

MATERIALS AND METHODS

Materials

In this work we used gelatin brand R-11 (molecular weight≈$4.9\cdot10^4$ g/mol)produced by TM Mriya, PJSC Ukroptbakalia, Ukraine, sodium alginate (molecular weight≈*216g/mol)* produced by Lianyungang Fengyun Seaweed Manufacturer Co.,Ltd., China, and aminocaproic acid powder produced by UmanHimTrade Co., Ukraine.

Methods

Sample Preparation

Humic acids were obtained by extraction from brown coal with a solution of sodium pyrophosphate and further extraction with 1% NaOH, followed by precipitation with hydrochloric acid as described in [19,20] and have a pH of 6.0. To prepare a gelatin-alginate hydrogel containing 14 wt.% GN and 6.4 wt.% ALG, the calculated mass of gelatin was first placed in distilled water, preheated to 90°C, and stirred with a VEVOR 85-2 magnetic stirrer in a water bath until a homogeneous gelatin sol was obtained. Sodium alginate was then added to the gelatin sol, and stirred with a magnetic stirrer to obtain a homogeneous sol, which, after cooling to room temperature, turned into a GN-ALG hydrogel, a photo of which is shown in Figure **1a**. To modify the GN-ALG hydrogel with humic acids, concentrated suspensions of HAs in aqueous solutions of 1 wt.% NaOH were used. These suspensions were added to the GN-ALG hydrogel in calculated amounts to obtain GN-ALG-HA2.5, GN-ALG-HA5 and GN-ALG-HA7.5 hydrogels containing 2.5 wt.% HA, 5 wt.% HA and 7.5 wt.% HA, respectively. Figure **1b, 1c** show photographs of the obtained GN-ALG-HA2.5 and GN-ALG-HA5 hydrogels, the color intensity of which increases with increasing humic acid content. To impregnate hydrogels with aminocaproic acid, 1.018 g of AA powder was added to 5 ml of a sol sample corresponding to each of the GN-ALG, GN-ALG-HA2.5 or GN-ALG-HA5 hydrogels heated to a temperature above 50°C and thoroughly mixed to obtain a suspension that after cooling, transformed into GN-ALG-AA, GN-ALG-HA2.5-AA, or GN-ALG-HA5-AA hydrogel, respectively. Photo of the GN-ALG-AA hydrogel shown in Figure **1d** demonstrates the incomplete dissolution of aminocaproic acid in the gelatin-alginate hydrogel.

Characterization

In this work, we took into account that an effective strategy for active hemostasis is the ability of the hydrogel to quickly absorb large amounts of water, which allows for rapid concentration coagulation factors from the blood with subsequent clot formation [13, 21, 22, 23, 24]. In addition, free swelling models the ability of hydrogels to absorb exudate at the wound site during the process of passive hemostasis [25, 26]. To evaluate the absorption capacity of hemostatic hydrogels during free swelling, molded hydrogel washers with a volume of 15 ml, a height of 0.9 cm, and a diameter of 5 cm each were used.

Measurements of the equilibrium degree of swelling (*EDS*) of hydrogels were carried out similarly to [15,25,26] according to the European standard EN 13726:2023 “Test methods for wound dressings - Aspects of absorption, moisture vapour transmission, water proofness and extensibility”.

To do this, a washer of dried hydrogel with mass W_d was immersed for 30 seconds in a Petri dish filled with distilled water or an aqueous solution of 142 mM NaCl and 2.5 mM $CaCl_2$, heated to physiological temperature (37 ± 1) °C, with a solution/hydrogel volume ratio of 40:1. According to Xie *et al*. (2022), the specified solution has an ionic composition comparable to human serum or wound exudate. After 30 seconds of swelling, the swollen mass of the hydrogel washer, W_s, was recorded. The equilibrium degree of swelling for each hydrogel was calculated as follows:

$$EDS,\% = (W_s - W_d) \times 100 / W_d \,, \quad (1)$$

According to Xi *et al*. (2019), the fluid absorption rate, called the swelling rate *SR* by the authors of Xi *et al*. (2019), for the non-porous hydrogel developed in this work was measured using a simple setup, a photo of which is shown in Figure **1e**. This setup consists of a Buchner funnel, a flexible tube and a graduated pipette. The graduated pipette is connected by a flexible tube to the outlet of the Buchner funnel and is positioned horizontally at the same height as the bottom of the Buchner funnel. During measurements at room temperature, distilled water was added to the Buchner funnel until the water level in the graduated pipette stabilized on a fixed scale. This position of the water volume was recorded as V_0. The molded hydrogel washer was then placed into a Buchner funnel as shown in Figure **1e**, and the water level in the graduated pipette began to move due to the swelling of the hydrogel. When the water level in the graduated pipette stabilized again, the time *t* and the final water volume V_1 were recorded. The swelling rate was calculated using the following equation [13]:

$$SR = 4(V_0 - V_1) / t\pi d^2 \,, \quad (2)$$

where *d* is the internal diameter of the Buchner funnel.

To identify crystalline regions in developed hemostatic hydrogels and to characterize nanocrystallites, X-ray diffraction analysis (XRD) was carried out on films of gelatin-alginate hydrogels,

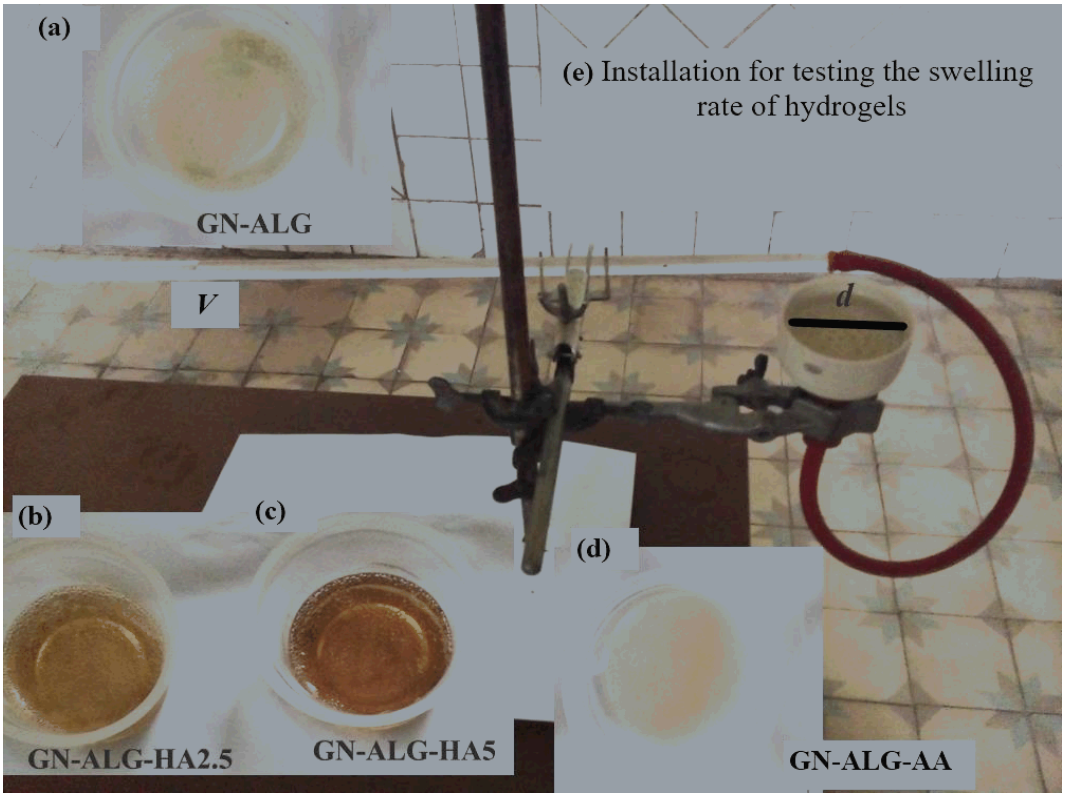

Figure 1: Photos of the GN-ALG hydrogel containing 14 wt.% GN and 6.4 wt.% ALG (**a**); hydrogel GN-ALG-HA2.5 containing 14 wt.% GN, 6.4 wt.% ALG and 2.5 wt.% HA (**b**); hydrogel GN-ALG-HA5 containing 14 wt.% GN, 6.4 wt.% ALG and 5 wt.% HA (**c**); hydrogel GN-ALG-AA containing 14 wt.% GN and 6.4 wt.% ALG and 1.018 g aminocaproic acid (~0.2 g/ml) (**d**). (**e**) – Photo of a setup for testing the swelling rate of hydrogels.

including those modified with humic acids, deposited on glass substrates and dried. For this purpose, we used a Shimadzu XRD-6100 diffractometer with monochromatic CuKα radiation (λ_x = 1.54060 Å) operating in the Bragg–Brentano geometry (θ–2θ). Using the "New_Profile v.3.4 (486)" program, the experimental X-ray diffraction patterns were processed by analytical methods to remove the background, smooth and split the Kα1 – Kα2 doublet. In addition, using the "New_Profile v.3.4 (486)" program, the parameters of diffraction profiles were calculated, including the correct determination of Bragg angles θ and the shape of Bragg peaks by decomposing complex profiles into components using the Gaussian approximation.

The X-ray line broadening method using the Scherer equation, as in [27], estimated the average size of nanocrystallites *D* in hydrogels:

$$D = (k \cdot \lambda_x) / (\beta \cdot \cos\theta), \quad (3)$$

where *k* = 0.9 is the Scherrer constant for spherical nanocrystals; *β* is the broadening of the Bragg peak at half maximum intensity (full width at half maximum, FWHM), obtained after processing the X-ray pattern using the "New_Profile v.3.4 (486)" program and subtracting the instrumental peak broadening, in radians.

The average distance between adjacent crystal planes, the interplanar spacing d_c, was calculated using Bragg's law and *n* = 1 [27]:

$$n\lambda_x = 2d_c \sin\theta \quad (4)$$

The dislocation density was estimated through $1/D^2$, according to Klochko *et al*. (2021).

To study the noncovalent interactions between GN, ALG, and HA in hemostatic hydrogels, we used Fourier transform infrared spectroscopy (FTIR). Fourier transform IR spectra were obtained on a Nicolet 380 IR spectrophotometer (USA) at a temperature of 25 °C in the frequency range 500-4000 cm^{-1}.

To simulate the delivery of aminocaproic acid from hemostatic hydrogels to a wound, a homemade setup was used in which white parchment paper was used as a semipermeable membrane covering one end of a glass pipe with an internal diameter of 50 mm. A molded hydrogel washer with a volume of 5 ml and a diameter of 50 mm, impregnated with ~0.2 g/ml aminocaproic acid, was placed on top of the membrane through the second open end of the glass pipe. Then, a glass pipe with a hydrogel on the surface of the membrane was immersed vertically for ten minutes in 45 ml of distilled water heated to physiological temperature (37±1)° or in 45 ml of an aqueous solution of 142 mM NaCl and 2.5 mM $CaCl_2$, similar in ionic composition to blood serum or wound exudate. Water molecules and salt ions from the solution penetrated through the semi-permeable membrane into the hydrogel, ensuring its swelling and complete dissolution of aminocaproic acid. Due to diffusion and osmosis, aminocaproic acid molecules penetrated the membrane and were transferred to distilled water or the solution contained 142 mM NaCl and 2.5 mM $CaCl_2$. The amount of aminocaproic acid released from the hydrogel and passed through the membrane was determined by acid-base titration of the resulting solution. To do this, 25 ml of acetone, 5 ml of water and 1 ml of 0.1% thymolphthalein indicator were added to the resulting solution and titrated with a sodium hydroxide solution 0.1 M NaOH until the resulting solution turned blue. The titration results were compared with a reference titration, according to which 1 ml of 0.1 M NaOH corresponds to 13.12 mg of AA. Experiments on the swelling of hemostatic hydrogels and their ability to deliver aminocaproic acid through a parchment paper membrane were performed in three replicates to ensure reproducibility. The obtained data were presented as average values and standard deviations. For statistical analysis, data normality was assessed by Tukey's multiple comparison post hoc test using ANOVA. The parameters used in the ANOVA analysis had a significance value of $p < 0.05$ at the 95% confidence level.

RESULTS AND DISCUSSION

X-ray diffraction patterns of the hemostatic hydrogels developed in this work are presented in Figure **2**. The gelatin-alginate hydrogel GN-ALG in Figure **2a** exhibits two peaks and an amorphous halo, which, according to literature data [25-31], belong predominantly biopolymer alginate anion, which is built from residues of β-D-mannuronic acid and α-Lguluronic acid. The presence of nanocrystalline regions in ALG is explained [33] by the strong interaction between alginate chains through intermolecular hydrogen bonds. According to Wang *et al*. (2017), the diffraction peak at Bragg angle 2θ of approximately 14º belongs to the (110) crystal plane of the *polyguluronate*segment(G), the peak at 2θ of approximately 22º belongs to the (200) crystal plane of the *polymannuronatesegment*(M), and the halo at an

angle 2θ of approximately 40° corresponds to the amorphous alginate phase. The authors Radev *et al*. (2009) described the structure of gelatin as almost amorphous with a halo at 2θ of about 20°. However, the authors Wang *et al*. (2017), Venezia *et al*. (2022), associate the broad X-ray diffraction peak at 2θ ≈ 20° with the partially crystalline structure of the GN explained by the presence of α-helix in the gelatin. Thus, in gelatin-alginate hydrogels, the diffraction peak at 2θ around 20° can also be attributed to the presence of GN nanocrystallites.

As X-ray diffraction analysis showed, the addition of humic acids did not lead to a fundamental change in the structure of gelatin-alginate hydrogels. When the HA content is no more than 2.5 wt.%, the number of nanocrystalline segments increases due to additional non-covalent bonds HA-GN and HA-ALG, which can be judged by the increase in the intensity of both (110)G and (200)M+GN peaks in Figure **2b**. A similar phenomenon of an increase in gel strength at low concentrations of HA in gelatin hydrogels was observed in [15].

However, higher addition of HA to the GN hydrogel in [15] resulted in a weaker gel because HA establishes preferential bonds with water molecules, preventing them from coordinating with the gelatin chains. The authors Venezia *et al*. (2022) showed that these features led to a change in the secondary structure of gelatin, which lost the triple-helix structure and exhibited an increase in the random coil conformation. In addition, higher mass content of HA caused swelling phenomena due to water absorption of HA, which contributed to the production of a weaker gel [15]. A similar decrease in hydrogel strength with the addition of large amounts of humic acids was observed in this work as a decrease in the degree of crystallinity of gelatin-alginate hydrogels.In Figure **2c, 2d**, and in Table **1**, it is clear that the addition of 5 wt.% and 7.5 wt.% humic acids, respectively, to the gelatin-alginate hydrogel reduces the number of nanocrystalline polyguuronate segments, as evidenced by a decrease in the intensity of the (110)G peak in the corresponding X-ray diffraction patterns at 2θ of approximately 14°.

The results of calculations using the Scherer formula (3), presented in Table **1** showed a decrease in the average size of nanocrystallites of polyguluronate units of alginate *D* from 5.3 nm to 2.3 nm with an increase in the concentration of HA in the gelatin-alginate hydrogel from 2.5 wt.% to 7.5 wt.%.

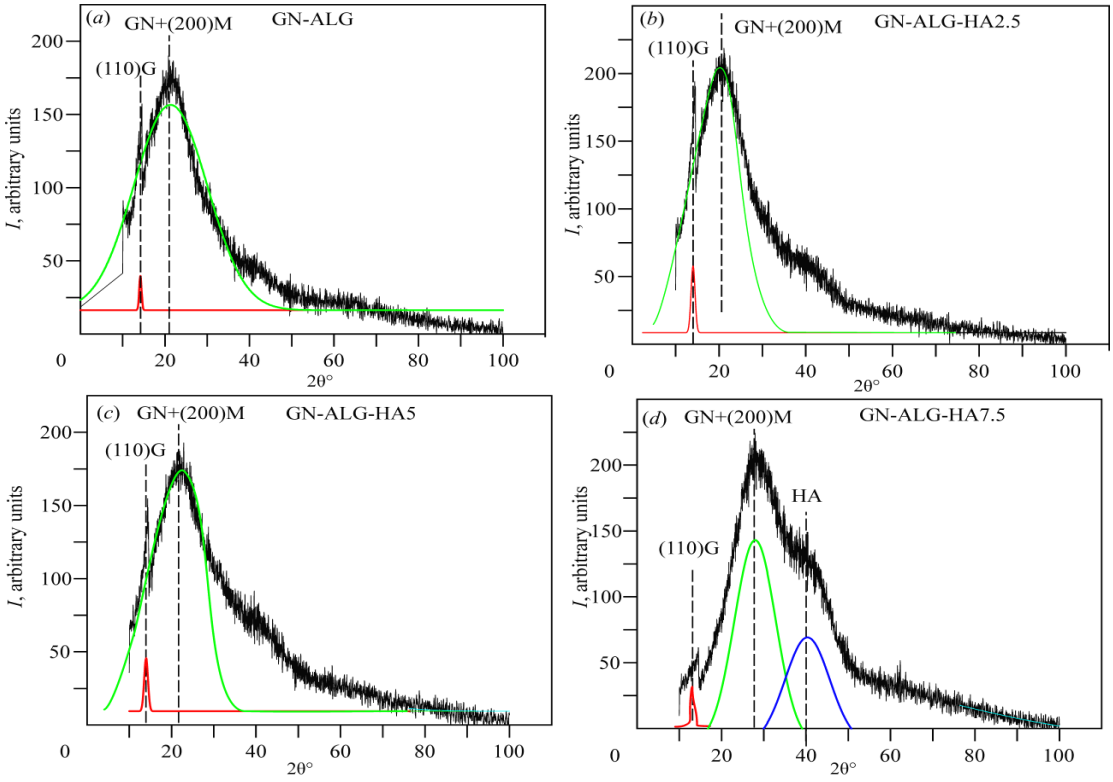

Figure 2: X-ray diffractions of dried gelatin-alginate hydrogel films on glass substrates: (**a**) GN-ALG; (**b**) GN-ALG-HA2.5; (**c**) GN-ALG-HA5; (**d**) GN-ALG-HA7.5. Red, green and blue lines mean decomposition of complex profiles into components using the Gaussian approximation.

Table 1: Analysis of the Nanocrystalline Structure of Gelatin-Alginate Hydrogels, including those Modified with Humic Acids, According to X-Ray Diffraction Data

Sample	(110) G plane of alginate				GN and (200)M plane of alginate			
	Position, 2θ, degree	Intensity, counts	Crystal size, *D*, nm	Dislocation density, $1/D^2$, line/nm^2	Position, 2θ, degree	Intensity, counts	Crystal size, *D*, nm	Dislocation density, $1/D^2$, line/nm^2
GN-ALG	14.54	28	5.3	0.04	20.82	140	0.68	2.16
GN-ALG-HA2.5	14.38	52	5.3	0.04	21.14	190	0.71	1.98
GN-ALG-HA5	14.34	39	3.6	0.08	22.86	165	0.66	2.30
GN-ALG-HA7.5	14.52	26	2.3	0.19	27.94	148	0.60	2.78

Accordingly, the dislocation density in the (110) plane of polyguuronate increased sharply from 0.04 to 0.19 lines/nm^2.

Moreover, analysis of the effect of HA on gelatin nanocrystals and the nanocrystalline polymannuronate component of alginate, i.e. on the GN+(200)M peak in X-ray diffractions (Figure **2c, 2d,** Table **1**) demonstrates a decrease in the interplanar distances d_c of gelatin and polymannuronate nanocrystals. In accordance with equation (4), this is evidenced by a shift of the GN+(200)M peak towards larger 2θ angles from approximately 21° for GN-ALG to almost 23° for GN-ALG-HA5 and to almost 28° for GN-ALG-HA7.5. The above confirms the occurrence of large tensile microstrains in small gelatin/polymannuronate nanocrystals with a *D* size of about 0.7 nm as a result of the addition of large amounts of humic acids to the gelatin-alginate hydrogel. Accordingly, the high dislocation density in these small nanocrystals increased further to 2.78 lines/nm^2, indicating the formation of a more disordered gel. In addition, as the concentration of humic acids in the gelatin-alginate hydrogel increases, the X-ray diffractions show an increase in amorphous halos at the 2θ angle of approximately 40°, which is due to the defective structure of the gelatin-alginate hydrogel aggravated by the addition of HA. At the concentration of humic acids of 7.5 wt.%, an additional peak is observed in the X-ray diffraction pattern (Figure **2d**) at 2θ ≈ 40°, which corresponds to small HA nanocrystals with *D* ~1 nmfound in the gelatin-alginate hydrogel.

FTIR analysis of the developed gelatin-alginate hydrogels confirms the intermolecular interactions shown for gelatin-alginate hydrogels in [33]. These include electrostatic interactions between the negatively charged COO^- groups of alginate and the positively charged NH_3^+ groups of gelatin. The electrostatic interactions can help shorten the bond length of the -NH functional groups, thereby increasing the wavenumber of the amide A band of 3306 cm^{-1} in gelatin [15], which is shifted to 3400 cm^{-1} in gelatin-alginate hydrogels GN-ALG, GN-ALG-HA2.5, GN-ALG-HA5 and GN-ALG-HA7.5.Figure **3** also shows asymmetric and symmetric ν_{CH2} vibrations of the amide region B of gelatin at 2853 cm^{-1} and 2930 cm^{-1}, previously described for gelatin and gelatin-alginate hydrogels in [13,33]. In addition, in all hydrogels developed in this work, the complexes are organized due to hydrogen bonds formed within and between the chains of biopolymers with the participation of their hydroxyl, carbonyl, carboxyl and amino groups. For example, the Amide I band of gelatin and the absorption band of alginate, attributed to the asymmetric stretching vibration of COO^-, are red-shifted and located at 1643 cm^{-1} and 1557 cm^{-1}, respectively, which is explained by the weakening of gelatin-gelatin and alginate-alginate chain interactions. In all developed hydrogels, the absorption band, assigned in gelatin hydrogel in [15] to the symmetric stretching vibration of COO^-, is shifted towards a higher wave number and is located at 1453 cm^{-1}. Similarly, the addition of ALG to GN led to a shift of the Amide III band (1238 cm^{-1}) in the gelatin spectrum towards higher wavenumbers – up to 1253 cm^{-1}. According to Bhagyaraj and Krupa (2020), the latter shift is also associated with an increase in the hydration of gelatin macromolecules and, in general, is caused by a change in the secondary structure of gelatin. In accordance with [31], sodium alginate leads to a decrease in the ordering of gelatin chains, i.e. in gelatin-alginate hydrogels, the proportion of triple helices decreases and, on the other hand, the content of random coil sections in the gelatin α-chain increases. At the same time, the absorption of $\nu_{c\text{-}o}$ vibrations in the mannuronic units of alginate is at the level of 1093 cm^{-1}, as in pure alginate hydrogel [35].

As can be seen from Figure **3**, in general, the position of the peaks in the FTIR spectra does not

change when humic acids are added to the gelatin-alginate hydrogel. The shapes of the FTIR spectra for GN-ALG, GN-ALG-HA2.5 and GN-ALG-HA5 are similar. However, in a gelatin-alginate hydrogel with an excess amount of humic acids GN-ALG-HA7.5, a significant change in the orientation of the molecules occurs, which is associated with changes in the polarization of vibrations that arise during the interaction of infrared irradiation with their dipole moments. This results in a weakening of the IR-active vibrations of the GN-ALG-NA7.5 hydrogel, which is clearly visible in Figure **3** by reducing characteristic absorption peaks.

Thus, as a result of studying the crystal structure by XRD and noncovalent interactions by FTIR, it was revealed that properties characteristic of hemostatic gelatin-alginate hydrogels or even improved are observed with the addition of bactericidal and anti-inflammatory humic acids in quantities in the range of 2.5-5 wt. %. Therefore, such hydrogels were subsequently used for impregnation with an additional hemostatic agent – amitnocaproic acid.

The above analysis of the crystal structure and intermolecular noncovalent bonding in hemostatic hydrogels corresponds very well with the results of assessing their free swelling absorption capacity at physiological temperature, presented in Table **2**. The experimentally obtained equilibrium degree of swelling of pure GN-ALG hydrogel is8.3± 0.1 %.In GN-ALG-HA2.5 *EDS* decreased to 6.1± 0.1 % as a result of increased gel strength at low HA concentrations, and *EDS* increased slightly to 7.1± 0.1 % in GN-ALG-HA5 as higher amounts of HA established preferential bonds with water molecules, preventing them from

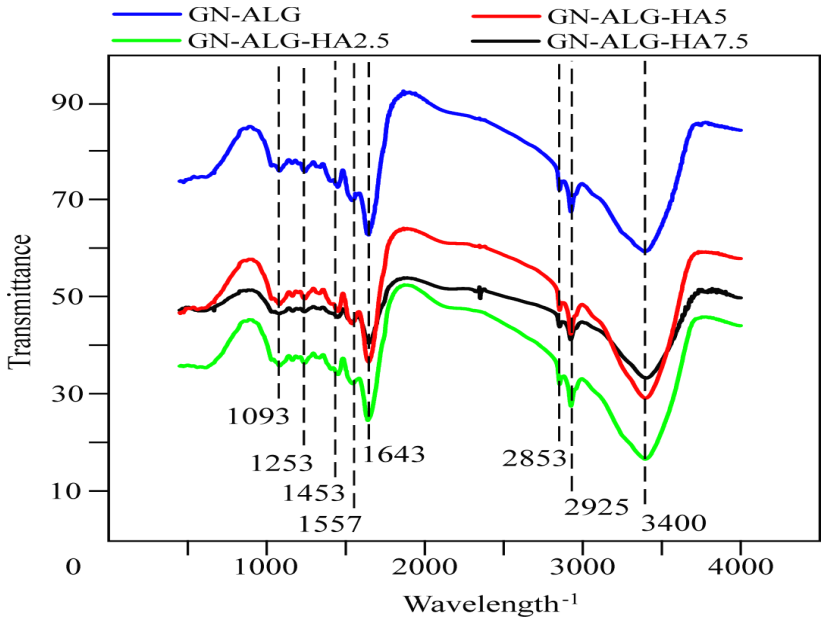

Figure 3: FTIR spectra of the developed hemostatic gelatin-alginate hydrogels, including those modified with humic acids.

Table 2: The Degree of Swelling of Hemostatic Hydrogels and their Ability to Deliver Aminocaproic Acid through A Parchment Paper Membrane at Physiological Temperature

Hydrogel	Equilibrium degree of swelling, *EDS*, %	Quantitative assessment of transmembrane transfer of aminocaproic acid, mg	
		In distilled water	In aqueous solution of 142 mM NaCl and 2.5 mM $CaCl_2$
GN-ALG	8.3± 0.1	-	-
GN-ALG-HA2.5	6.1± 0.1	-	-
GN-ALG-HA5	7.1± 0.1	-	-
GN-ALG-AA	19.8± 0.2	182 ± 2	195 ± 3
GN-ALG-HA2.5-AA	27.2± 0.2	276± 3	282± 4
GN-ALG-HA5-AA	26.8± 0.1	468± 2	494± 3

coordinating with gelatin chains. Accordingly, swelling rate studies showed high *SR* values for the developed hydrogels: 0.87± 0.01 ml/(s·cm^2), 0.71± 0.01ml/(s·cm^2) and 0.66 ± 0.01ml/(s·cm^2) for GN-ALG, GN-ALG-HA2.5 and GN-ALG-HA5, respectively.

Due to the hydrophilicity of aminocaproic acid, the swelling ability at physiological temperature of the developed hemostatic gelatin-alginate hydrogels impregnated with aminocaproic acid, especially those modified with humic acids, sharply increased. The experimentally studied equilibrium degree of swelling in the GN-ALG-AA hydrogel is 19.8± 0.2 %, in GN-ALG-HA2.5-AA it increases to 27.2± 0.2 %, and in GN-ALG-HA5-AA *EDS* ≈ 26.8± 0.1 % (Table **2**).

Quantification of the transmembrane transport of aminocaproic acid from the developed gelatin-alginate hydrogels at physiological temperature, shown in Table **2**, confirms their excellent suitability for delivering this effective hemostatic agent to the wound. In experiments with the GN-ALG-AA hydrogel, it was found that 182±2 mg of AA pass through the pores of parchment paper into water and 195± 3 mg of AA pass into a solution with an ionic composition close to blood serum and wound exudate (Table **2**).

It should be noted that when using in control experiments the same amount of dry aminocaproic acid as in the GN-ALG-AA hydrogel, the transition of AA through a parchment paper membrane in the amount of 190 ± 1 mg into water and 197± 2 mg into the specified solution was observed, that is, not much more than from gelatin-alginate hydrogel. The reason is that the hemostatic gelatin-alginate hydrogels developed in this work are thermo-responsive and have a gel-sol transition temperature close to physiological, at which intramolecular and intermolecular bonds are weakened, due to which the hemostatic material can penetrate the uneven and deep surfaces of wounded tissues, where aminocaproic acid is easily released. The more intense transition of aminocaproic acid through the membrane into a saline solution rather than into water is explained by the phenomenon of osmosis. Moreover, when using gelatin-alginate hydrogels impregnated with aminocaproic acid and modified with humic acids, the transmembrane transfer of aminocaproic acid occurred especially intensively, which can be explained by the particularly high equilibrium degrees of swelling of such hydrogels, shown in Table **2**. Thus, according to experimental data, the hemostatic hydrogels developed in this work make it possible to quickly deliver to the wound about a third of the amount of aminocaproic acid contained in GN-ALG-HA2.5-AA and about half of the aminocaproic acid contained in GN-ALG-HA5-AA.

CONCLUSIONS

In this work, studies of the crystal structure and intermolecular interactions in the developed hemostatic gelatin-alginate hydrogels modified with bactericidal and anti-inflammatory humic acids made it possible to identify optimal HA concentrations from 2.5 to 5 wt.%. At these concentrations of HA, hydrogels have a semicry stalline structure and noncovalent interactions of polymer chains, due to which they are thermo-responsive with a gel-sol transition temperature of about 37 °C and, thus, are able to melt on the wound surface and penetrate into deep wounds to access the source of bleeding. Moreover, these hydrogels have been experimentally shown to have a high swelling rate and swelling ability, allowing the initiation of a blood clotting cascade within 30 seconds of application to a bleeding wound. In order to create safe and biocompatible multicomponent hemostatic materials based on biopolymers with an enhanced hemostatic effect due to antifibrinolysis, these hydrogels were impregnated with aminocaproic acid that increased approximately four fold their swelling, which contributed to the dissolution of AA in hydrogels and its subsequent delivery to the wound. Experiments simulating the transmembrane transport of aminocaproic acid from the developed gelatin-alginate hydrogels confirm their ability to rapidly deliver 282± 4 mg of AA from 5 ml of GN-ALG-HA2.5-AA hydrogel and 494± 3 mg of AA from 5 ml of GN-ALG-HA2.5-AA hydrogel to the wound.

Terminal sterilization of composite biomaterials is crucial for their use in hemostasis and wound healing. It is necessary to obtain regulatory approval and to safely proceed to clinical trials [36-39]. However, according to Galante *et al*. (2018), Stoppel *et al*. (2014), Zhang *et al*. (2022), sterilization of biopolymer hydrogels is particularly challenging due to the well-known sensitivity of this type of material to common sterilizing agents such as heat and radiation. It is noted by Galante *et al*. (2018), Zhang *et al*. (2022), Carranza *et al*. (2023), that the impact of sterilization methods on the internal properties of systems based on biopolymer hydrogels has not been sufficiently studied and further research is needed. Moreover, each system requires individual testing to select the most suitable and effective sterilization method, which will keep the basic properties unchanged [36-39]. Therefore, the next step in our research will be the careful selection of an

appropriate terminal sterilization method. Based on the experience of the authors of works [36-39], a proprietary sterilization method will be developed and optimized for hemostatic gelatin-alginate hydrogels modified with humic acids and impregnated with aminocaproic acid, including UV irradiation (250 nm) and air-plasma treatment.

REFERENCES

[1] Chen X-J, Lei Z-Y, Liu P, *et al.* An aminocaproic acid-grafted chitosan derivative with superior antibacterial and hemostatic properties for the prevention of secondary bleeding. Carbohydrate Polymers 2023; 316: 120988-11. https://doi.org/10.1016/j.carbpol.2023.120988

[2] Li Q, Hu E, Yu K, *et al.* Self-propelling Janus particles for hemostasis in perforating and irregular wounds with massive hemorrhage. Adv. Funct. Mater 2020; 30(42): 2004153-13. https://doi.org/10.1002/adfm.202004153

[3] Zhong Y, Hu H, Min N, *et al.* Application and outlook of topical hemostatic materials: A narrative review. Ann Transl Med 2021; 9(7): 577-20. https://doi.org/10.21037/atm-20-7160

[4] Jiao S, Zhang X, Cai H, *et al.* Recent advances in biomimetic hemostatic materials. Materials Today Bio 2023; 19: 100592-22. https://doi.org/10.1016/j.mtbio.2023.100592

[5] Yang X, Wang X, Gao X, *et al.* What else should hemostatic materials do beyond hemostasis: A review. Materials Today Bio 2024; 25: 101008-18. https://doi.org/10.1016/j.mtbio.2024.101008

[6] Ghimire S, Sarkar P, Rigby K, *et al.* Polymeric materials for hemostatic wound healing. Pharmaceutics 2021; 13: 2127-27. https://doi.org/10.3390/pharmaceutics13122127

[7] Yu P, Zhong W. Hemostatic materials in wound care. Burns & Trauma 2021: 9; tkab019-17. https://doi.org/10.1093/burnst/tkab019

[8] Peng X, Xu X, Deng Y, *et al.* Ultrafast self-gelling and wet adhesive powder for acute hemostasis and wound healing. Adv. Funct. Mater 2021; 31(33): 2102583-13. https://doi.org/10.1002/adfm.202102583

[9] Xie Y, Gao P, He F *et al.*Application of alginate-based hydrogels in hemostasis Gels 2022; 8: 109-21. https://doi.org/10.3390/gels8020109

[10] Fatimi A. Cellulose-Based Hydrogels: Patent Analysis. Journal of Research Updates in Polymer Science 2022; 11: 16–24. https://doi.org/10.6000/1929-5995.2022.11.03

[11] Karim MM, Lasker T, *et al.* Low-Cost Production of Chitosan Biopolymer from Seafood Waste: Extraction and Physiochemical Characterization. Journal of Research Updates in Polymer Science 2024; 13: 17–26. https://doi.org/10.6000/1929-5995.2024.13.03

[12] Du Y, Li L, Peng H, *et al.* A spray-filming self-healing hydrogel fabricated from modified sodium alginate and gelatin as a bacterial barrier. Macromol. Biosci 2020; 20: 1900303-11. https://doi.org/10.1002/mabi.201900303

[13] Xi G, Liu W, Chen M, *et al.* Polysaccharide-based lotus seedpod surface-like porous microsphere with precise and controllable micromorphology for ultrarapid hemostasis. ACS Appl. Mater. Interfaces 2019; 11: 46558−46571. https://doi.org/10.1021/acsami.9b17543

[14] Mecwan M, Li J, Falcone N, *et al.* Recent advances in biopolymer-based hemostatic materials. Regenerative Biomaterials 2022; 9: rbac063-26. https://doi.org/10.1093/rb/rbac063

[15] Venezia V, Avallone PR, Vitiello G, *et al.* Adding humic acids to gelatin hydrogels: a way to tune gelation. Biomacromolecule 2022; 23(1): 443–453. https://doi.org/10.1021/acs.biomac.1c01398

[16] Zeigler ZR. Effects of epsilon aminocaproic acid on primary hemostasis. Haemostasis 1991; 21(5): 313–320. https://doi.org/10.1159/000216242

[17] Heidmann P, Tornquist SJ, Qu A, *et al.* Laboratory measures of hemostasis and fibrinolysis after intravenous administration of □-aminocaproic acid in clinically normal horses and ponies. AJVR 2005; 66(2): 313–318. https://doi.org/10.2460/ajvr.2005.66.313

[18] Wilson JM, Bower LK, Fackler JC, Beals DA, Bergus BO, Kevy SV. Aminocaproic acid decreases the incidence of intracranial hemorrhage and other hemorrhagic complications of ECMO. Journal of Pediatric Surgery 1993; 28(4): 536–540. https://doi.org/10.1016/0022-3468(93)90612-O

[19] Lebedev V, Miroshnichenko D, Tykhomyrova T, *et al.* Design and research of environmentally friendly polymeric materials modificated by derivatives of coal. Petroleum and Coal 2023; 65(2): 334-340. https://doi.org/10.1063/5.0119925

[20] Lebedev V, Miroshnichenko D, Vytrykush N, *et al.* Novel biodegradable polymers modified by humic acids. Materials Chemistry and Physics 2024; 313: 128778. https://doi.org/10.1016/j.matchemphys.2023.128778

[21] Lebedeva KO, Cherkashina AM, Tykhomyrova TS, *et al.* Design and researching of biologically active polymeric hydrogel transdermal materials modified by humic acid. IOP Conference Series: Earth and Environmental Science 2023; 1254(1): 012009. https://doi.org/10.1088/1755-1315/1254/1/012009

[22] Lebedeva K, Cherkashina A, Voronkin A, *et al.* Design and researching smart biologically active polymeric hydrogel transdermal nanomaterial's. 2023 IEEE 4th KhPI Week on Advanced Technology (KhPIWeek) 2023: 1–5. https://doi.org/10.1109/KhPIWeek61412.2023.10312985

[23] Lebedeva K, Cherkashina A, Masikevych YG, *et al.* Modeling of Smart Bio-Medical Active Polymeric Hydrogel Transdermal Materials. Journal of Engineering Sciences 2024; 11(1): C1 - C7. https://doi.org/10.21272/jes.2024.11(1).c1

[24] Miroshnichenko D, Lebedeva K, Cherkashina A, *et al.* Study of hybrid modification with humic acids of environmentally safe biodegradable hydrogel films based on hydroxypropyl methylcellulose. C- Journal of carbon research 2022; 8: 71–10. https://doi.org/10.3390/c8040071

[25] Perkasa DP, Erizal E, Purwanti T, *et al.* Characterization of semi-interpenetrated network alginate/gelatin wound dressing crosslinked at sol phase. Indonesian Journal of Chemistry 2018; 18(2): 367–375. https://doi.org/10.22146/ijc.25710

[26] Uttayarat P, Chiangnoon R, Eamsiri J, *et al.* Processing and characterization of antibacterial hydrogel sheet dressings composed of poly(vinyl alcohol) and silk fibroin for wound healing application. Walailak J Sci & Tech 2019; 16(5): 349-359. https://doi.org/10.48048/wjst.2019.6292

[27] Klochko NP, Barbash VA, Petrushenko SI, *et al.* Thermoelectric textile devices with thin films of nanocellulose and copper iodide. Journal of Materials Science: Materials in Electronics 2021; 32: 23246–23265. https://doi.org/10.1007/s10854-021-06810-9

[28] Lan L, Ping J, Xiong J, *et al.* Sustainable natural bio-origin materials for future flexible devices. Adv. Sci. 2022; 9(15): 2200560–34. https://doi.org/10.1002/advs.202200560

[29] Sundarrajan P, Eswaran P, Marimuthu A, *et al.* One pot synthesis and characterization of alginate stabilized semiconductor nanoparticles". Bull. Korean Chem. Soc. 2012; 33(10): 3218–3224. https://doi.org/10.5012/bkcs.2012.33.10.3218

[30] Ghosh D, Pramanik A, Sikdar N, *et al.* Synthesis of low molecular weight alginic acid nanoparticles through persulfate treatment as effective drug delivery system to manage drug resistant bacteria", BiotechnolBioproc E 2011; 16: pp. 383-392. https://doi.org/10.1007/s12257-010-0099-7

[31] Bhagyaraj S, Krupa I. Alginate-mediated synthesis of hetero-shaped silver nanoparticles and their hydrogen peroxide sensing ability. Molecules 2020; 25: 435-10. https://doi.org/10.3390/molecules25030435

[32] Radev L, Fernandes M, Salvado I, *et al.* Organic/inorganic bioactive materials Part III: *in vitro* bioactivity of gelatin/silicocarnotite hybrids. Open Chemistry 2009; 7(4): 721-730. https://doi.org/10.2478/s11532-009-0078-z

[33] Wang K, Wang W, Ye R, *et al.* Mechanical and barrier properties of maize starch-gelatin composite films: effects of amylose content. J Sci Food Agric. 2017; 97(11): 3613-3622. https://doi.org/10.1002/jsfa.8220

[34] Koesnarpadi S, Santosa SJ, Siswanta D, *et al.* Synthesis and characterization of magnetite nanoparticle coated humic acid (Fe3O4/HA). Procedia Environmental Sciences 2015; 30: 103 – 108. https://doi.org/10.1016/j.proenv.2015.10.018

[35] Derkach SR, Voron'ko NG, Sokolan NI, *et al.* Interactions between gelatin and sodium alginate: UV and FTIR studies. Journal of Dispersion Science and Technology 2019; 5: 690-698. https://doi.org/10.1080/01932691.2019.1611437

[36] Galante R, Pinto TJA, Colaço R, *et al.* Sterilization of hydrogels for biomedical applications: A review. J Biomed Mater Res Part B 2018; 106(6): 2472-2492. https://doi.org/10.1002/jbm.b.34048

[37] Stoppel WL, White JC, Horava SD, *et al.* Terminal sterilization of alginate hydrogels: Efficacy and impact on mechanical properties. J Biomed Mater Res Part B 2014; 102Ba: 877–884. https://doi.org/10.1002/jbm.b.33070

[38] Zhang F, Scull G, Gluck JM, *et al.* Effects of sterilization methods on gelatin methacryloyl hydrogel properties and macrophage gene expression *in vitro*. Biomed Mater. 2022; 18(1): 10-27. https://doi.org/10.1088/1748-605X/aca4b2

[39] Carranza T, Zalba- Balda M, BarriolaBaraibar MJ, *et al.* Effect of sterilization processes on alginate/gelatin inks for three-dimensional printing. Int J Bioprint, 2023; 9(1): 309-319. https://doi.org/10.18063/ijb.v9i1.645

Received on 16-06-2024 Accepted on 15-07-2024 Published on 05-08-2024

https://doi.org/10.6000/1929-5995.2024.13.05